

CERN-TH-2002-170
 IFUM-716/FT
 FTUAM-02-378

Determination of Neutrino mixing parameters after SNO oscillation evidence

P. Aliani^{a*}, V. Antonelli^{a*}, M. Picariello^{a*}, R. Ferrari^{a*}, E. Torrente-Lujan^{abc*}

^a *Dip. di Fisica, Univ. di Milano and INFN Sezione di Milano,
 Via Celoria 16, Milano, Italy*

^b *Dept. Fisica Teorica C-XI, Univ. Autonoma de Madrid, 28049 Madrid, Spain,*

^c *CERN TH-Division, CH-1202 Geneve*

Abstract

An updated analysis of all available neutrino oscillation evidence in Solar experiments (SK day and night spectra, global rates from Homestake, SAGE and GALLEX) including the latest *SNOCC* and *NC* data is presented. Assuming that the shape of the SNO CC energy spectrum is undistorted and using the information provided by SNO we obtain, for the fraction of electron neutrinos remaining in the solar beam at energies $\gtrsim 5$ MeV:

$$\phi_{CC}/\phi_{NC} = 0.34^{+0.05}_{-0.04},$$

which is nominally $\sim 30\sigma$ away from the standard value ($\sim 1.8 \pm 0.1$). The fraction of oscillating neutrinos which into active ones is computed to be:

$$(\Phi_{NC} - \Phi_{CC})/(\Phi_{SSM} - \Phi_{CC}) = 0.92^{+0.39}_{-0.20}$$

nearly 5σ deviations from the pure sterile oscillation case. The data is still compatible with an important fraction of sterile component in the solar beam (up to 20% of the total).

In the framework of two active neutrino oscillations we determine individual neutrino mixing parameters and their errors in the region of no spectrum distortion ($\Delta\langle T_e \rangle < 1\%$), we obtain

$$\Delta m^2 = 4.5^{+2.7}_{-1.4} \times 10^{-5} \text{ eV}^2, \quad \tan^2 \theta = 0.40^{+0.10}_{-0.08}.$$

This is in agreement with the best *chi*² solution in the LMA region.

PACS: * email: paul@lcm.mi.infn.it, vito.antonelli@mi.infn.it, marco.picariello@mi.infn.it, torrente@cern.ch

1. Observation of neutral current neutrino interactions on deuterium in the SNO experiment has been recently presented [1]. Using the NC, ES and CC reactions and assuming the 8B neutrino shape predicted by the SSM, the electron and active non-electron component of the solar flux at high energies ($>\sim 5$ MeV) are obtained. The non-electron component is found to be $\sim 5\sigma$ greater than zero, the standard prediction, thus providing the strongest evidence so far for flavour oscillation in the neutral lepton sector: the agreement of the total flux, provided by the NC measurement with the expectations implies as a by-product the confirmation of the validity of the SSM [11–13].

The *SNO* experiment measures the 8B Solar neutrinos via the reactions [14–17]: 1) Charged Current (CC): $\nu_e + d \rightarrow 2p + e^-$, 2) Elastic Scattering (ES): $\nu_x + e^- \rightarrow \nu_x + e^-$. 3) Neutral Current(NC): $\nu_x + d \rightarrow p + n + \nu_x$. The first reaction is sensitive exclusively to electron neutrinos. The second, the same as the one used in SuperKamiokande (SK), is instead sensitive, with different efficiencies, to all flavours. Finally the NC reaction is equally sensitive to all active neutrino species.

The results presented recently by *SNO* on Solar neutrinos [10] confirm and are consistent with previous evidence from SK and other experiments [4, 6, 7, 18]. The CC, ES and NC global and day and night fluxes presented in Refs. [1, 2], summarised in Table 1, are derived under the assumption that the 8B spectral shape is not distorted from the SSM prediction. With this assumption the SNO collaboration checks the hypothesis of non-oscillation, or zero $\phi_{\mu+\tau}$ flux.

It would be advantageous to use this assumption of non-distortion for several reasons. Not only in general terms of simplicity and logical economy but also because with it a much higher statistical accuracy and power of prediction can be obtained (compare the total NC fluxes obtained with and without the distortion hypothesis obtained in [1]). Using these fluxes is appropriate for the calculation of constraints on mixing parameters in theoretical models where such spectrum distortion is negligible, this is true in particular for ample regions of oscillation space favoured by all previous data (with or without previous SNO CC data).

Usually, the best fit to the data has been routinely obtained in the LMA region (see [8] and references therein), the qualitative explanation for that being the fact that just in that region the observed rather undistorted SK spectrum can be optimally adjusted. The spectrum distortion of the oscillating solutions for SNO in the LMA region has been explicitly found to be negligible [38]. Quantitatively, the main information content of the shape of the observable spectrum is summarised by the first moment of the distribution, the average spectrum energy. For the SSM case and in absence of oscillations, it is found in Ref.[38] that the average kinetic energy $\langle T_e \rangle = 7.658 \pm 0.006$ MeV. This is to be compared with the close expected value for a typical, non distorting, LMA oscillating solution $\langle T_e \rangle = 7.654$ MeV and with the far values of the distorted SMA (7.875 MeV) and VAC (8.361 MeV) solutions.

In this work we present an up-to-date analysis of all available Solar neutrino evidence including latest SNO results in the most simple framework. First we will reobtain some model independent results which put in a quantitative foot the extent of the deviations with respect

the standard non-oscillating case and the relative importance of active/sterile oscillations. Second we will obtain allowed area in parameter space in the framework of active two neutrino oscillations from a standard statistical analysis. Individual values for Δm^2 and $\tan^2 \theta$ with error estimation will be obtained from the analysis of marginal likelihoods. In this statistical analysis we include all available data from SK, Homestake and Gallium experiments. From SNO we include the latest results on global day and night fluxes, we make use in particular of: a) the total ${}^8\text{B}$ flux as measured by the NC reaction and b) the electron neutrino day-night global asymmetry. The main conclusion of our analysis to be presented below is that is already possible to determine at present active two neutrino oscillation parameters with relatively good accuracy.

2. Different quantities can be defined in order to make the evidence for disappearance and appearance of the neutrino flavours explicit. Letting alone the SNO data, from the three fluxes measured by SNO is possible to define two useful ratios, deviations of these ratios with respect their standard value are powerful tests for occurrence of new physics. Here we compute the values for ϕ_{CC}/ϕ_{ES} and ϕ_{CC}/ϕ_{NC} being specially careful with the treatment of the correlations on the uncertainties, the inclusion or not of these correlations can affect significantly their results. For the first ratio the value from SNO rates we obtain

$$\frac{\phi_{CC}}{\phi_{ES}} = 0.73^{+0.10}_{-0.07},$$

a value which is $\sim 2.7 \sigma$ away from the no-oscillation expectation value of one. The ratio of CC and NC fluxes gives the fraction of electron neutrinos remaining in the solar neutrino beam, our value is:

$$\frac{\phi_{CC}}{\phi_{NC}} = 0.34^{+0.05}_{-0.04},$$

this value is nominally many standard deviations ($\sim 30\sigma$) away from the standard model case ($\phi_{CC}/\phi_{NC} = 1.88 \pm 0.08$ from Ref.[38]).

Finally, if in addition to SNO data we consider the flux predicted by the solar standard mode one can define, following Ref.[19], the quantity $\sin^2 \alpha$, the fraction of "oscillation neutrinos which oscillated into active ones", again using the SNO data and fully applying systematic correlations (see table 2 in Ref. [1]), we find the following result:

$$\sin^2 \alpha = \frac{\Phi_{NC} - \Phi_{CC}}{\Phi_{SSM} - \Phi_{CC}} = 0.92^{+0.39}_{-0.20}.$$

The SSM flux is taken as the ${}^8\text{B}$ flux predicted in Ref.[12]. Note that, although consistent with it, this result differs significantly from the number obtained in Ref.[19], this is due to the introduction of systematic correlations in our calculation. The central value is clearly below one (only-active oscillations). Although electron neutrinos are still allowed to oscillate into sterile neutrinos the hypothesis of transitions to *only* sterile neutrinos is rejected at nearly 5σ , this significance would be reduced approximately by half if we consider apply a 1-sided analysis to avoid non-physical values.

3. Our determination of neutrino oscillations in Solar and Earth matter and of the expected signal in each experiment follows the standard methods found in the literature [22]. As is explained in detail in Ref.[8], for this analysis we completely solve numerically the neutrino equations of evolution for all the oscillation parameter space. The survival probabilities for an electron neutrino, produced in the Sun, to arrive at the Earth are calculated in three steps. The propagation from the production point to Sun's surface is computed numerically in all the parameter range using the electron number density n_e given by the BPB2001 model [12] averaging over the production point. The propagation in vacuum from the Sun surface to the Earth is computed analytically. The averaging over the annual variation of the orbit is also exactly performed using simple Bessel functions. To take the Earth matter effects into account, we adopt a spherical model of the Earth density and chemical composition. In this model, the Earth is divided in eleven radial density zones [23], in each of which a polynomial interpolation is used to obtain the electron density. The gluing of the neutrino propagation in the three different regions is performed exactly using an evolution operator formalism [22]. The final survival probabilities are obtained from the corresponding (non-pure) density matrices built from the evolution operators in each of these three regions. The night quantities are obtained using appropriate weights which depend on the neutrino impact parameter and the sagitta distance from neutrino trajectory to the Earth center, for each detector's geographical location.

The expected signal in each detector is obtained by convoluting neutrino fluxes, oscillation probabilities, neutrino cross sections and detector energy response functions. We have used neutrino-electron elastic cross sections which include radiative corrections [24]. Neutrino cross sections on deuterium needed for the computation of the SNO measurements are taken from [25]. Detector effects are summarised by the respective response functions, obtained by taking into account both the energy resolution and the detector efficiency. The resolution function for SNO is that given in [1–3]. We obtained the energy resolution function for SK using the data presented in [26–28]. The effective threshold efficiencies, which take into account the live time for each experimental period, are incorporated into our simulation program. They are obtained from [32].

The statistical significance of the neutrino oscillation hypothesis is tested with a standard χ^2 method which is explained in detail in Ref.[8]. Our present analysis is based on the consideration of the following χ^2 quantity made of three well differentiated pieces:

$$\chi^2 = \chi_{\text{glob}}^2 + \chi_{\text{spec-sk}}^2 + \chi_{\text{SNO}}^2. \quad (1)$$

The contribution of SNO to the χ^2 is given by

$$\chi_{\text{SNO}}^2 = \left(\frac{\alpha - \alpha^{\text{th}}}{\sigma_\alpha} \right)^2 + \left(\frac{A_e^{\text{th}} - A_e^{\text{exp}}}{\sigma_A} \right)^2, \quad (2)$$

We have introduced the flux normalisation factor α with respect to the SNO NC flux whose central and error values are given in Table 1. This flux normalisation will be used below as

a scale factor for the SK spectrum. The quantity A_e is the asymmetry on the day and night electron neutrino rates extracted from the SNO CC, ES and NC data, imposing the condition $A_{tot} = A_{e+\mu\tau} \equiv 0$, as predicted by active-only models [2]. The strong anticorrelation of A_e and A_{tot} makes the imposition of this constraint useful, thus reducing greatly the uncertainties with respect to the raw A_{CC} .

The definition of the χ^2_{glob} function is the following:

$$\chi^2_{\text{glob}} = (\mathbf{R}^{\text{th}} - \mathbf{R}^{\text{exp}})^T (\sigma^2)^{-1} (\mathbf{R}^{\text{th}} - \mathbf{R}^{\text{exp}}) \quad (3)$$

where σ^2 is the full covariance matrix made up of two terms, $\sigma^2 = \sigma_{\text{unc}}^2 + \sigma_{\text{cor}}^2$. The diagonal matrix σ_{unc}^2 contains the theoretical, statistical and uncorrelated errors while σ_{cor}^2 contains the correlated systematic uncertainties. The $\mathbf{R}^{\text{th,exp}}$ are length 2 vectors containing the theoretical and experimental data normalised to the SSM expectations. The 2×2 correlation matrix have been computed using standard techniques [29, 30]. We have used data on the total event rates measured at Homestake experiment, at the gallium experiments SAGE [7, 33], GNO [20] and GALLEX [21] (see Table (1) for an explicit list of results and references). For the purposes of this work it is enough to summarise all the gallium experiments in one single quantity by taking the weighted average of their rates.

For the analysis of the SK energy spectrum, following closely the procedure assumed by the SK collaboration [31, 32], we consider a χ^2 function:

$$\chi^2_{\text{spec}} = \sum_{d,n} (\alpha \mathbf{R}^{\text{th}} - \mathbf{R}^{\text{exp}})^t (\sigma_{\text{unc}}^2 + \delta_{\text{cor}} \sigma_{\text{cor}}^2)^{-1} (\alpha \mathbf{R}^{\text{th}} - \mathbf{R}^{\text{exp}}) + \chi^2_{\delta}. \quad (4)$$

Where the vectors of data and expectations \mathbf{R} are defined as before. We have introduced the SNO NC flux normalisation factor α given above and the correlation parameter δ_{cor} is assumed to be constrained by the last term in the sum: $\chi^2_{\delta} = (\delta_{\text{cor}} - \delta_{\text{cor}}^{\text{th}})^2 / \sigma_{\delta}^2$. The complete variance matrix is not a constant quantity. It is obtained from combining the statistical variances with systematic uncertainties and dependent on this correlation parameter. For each day and night spectrum the corresponding 19×19 block correlation matrices are conservatively constructed assuming full correlation among energy bins. The components of the variance matrix are given by standard expressions [8] in terms of statistic errors, bin-correlated and uncorrelated uncertainties. The data and errors for individual energy bins for SK spectrum has been obtained from Ref. [32]. Other information from the SK results, such as the global day-night asymmetries, is to a large extent already contained in the above-mentioned quantities. It is therefore not included in our analysis and does not change the results presented further on.

4. To test a particular oscillation hypothesis against the parameters of the best fit and obtain allowed regions in parameter space we perform a minimisation of the four dimensional function $\chi^2(\Delta m^2, \tan^2 \theta, \alpha, \delta_{\text{cor}})$. For $\delta_{\text{cor}} = \delta_{\text{cor}}^{\text{min}}, \alpha = \alpha_{\text{min}}$, a given point in the oscillation parameter space is allowed if the globally subtracted quantity fulfils the condition $\Delta\chi^2 = \chi^2(\Delta m^2, \theta) - \chi^2_{\text{min}} < \chi^2_{n=4}(90\%, 95\%, \dots) = 7.78, 9.4, \dots$ are the quantiles for

four degrees of freedom. The χ^2 summation now contains 41 bins in total: 3 from the global rates and SNO asymmetry and 2×19 bins for the SK day and night spectrums.

The results are shown in Fig.1(left) where we have generated acceptance contours in Δm^2 and $\tan^2 \theta$. In Table (2) we present the best fit parameters or local minima obtained from the minimisation of the χ^2 function given in Eq. (3). Also shown are the values of χ^2_{\min} per degree of freedom (χ^2/n) and the goodness of fit (g.o.f.) or significance level of each point (definition of SL as in Ref. [34]). In Fig.1(right) we superimpose the global signal expected in the KamLAND experiment from reactor electron antineutrinos. We observe that at the most favoured regions obtained before, the KamLAND expected signal is situated at a intermediate region where high sensibility to both mass squared and mixing angle parameters is found. The experiment expects around 50% of the non-oscillation signal, in this region it would suffice to reach a total error of 5 – 10% (a quantity reachable after one year of data taking) in the measurement to be able to confirm the SNO results.

In order to obtain concrete values for the individual oscillation parameters and estimates for their uncertainties, it is preferable to study the marginalized parameter constraints. It is justified to convert χ^2 into likelihood using the expression $\mathcal{L} = e^{-\chi^2/2}$, this normalised marginal likelihood is plotted in Figs. (2) for each of the oscillation parameters Δm^2 and $\tan^2 \theta$. For $\tan^2 \theta$ we observe that the likelihood function is concentrated in a region $0.2 < \tan^2 \theta < 1$ with a clear maximum at $\tan^2 \theta \sim 0.4$. The situation for Δm^2 is similar. Values for the parameters are extracted by fitting one- or two-sided Gaussian distributions to any of the peaks. In the case of the angle distribution the goodness of fit of the Gaussian fit is excellent (g.o.f > 99.9%) even at far tail distances thus justifying the consistency of the procedure. The goodness of Gaussian fit to the distribution in squared mass, although somewhat smaller, is still good. The values for the parameters appear in Table 2. They are fully consistent and very similar to the values obtained from simple χ^2 minimisation.

In summary, in this work we have present an up-to-date analysis of all avaialble Solar neutrino evidence including latest SNO results in the most simple framework. The direct measurement via *NC* reaction on deuterium of $\phi_{^8\text{B}}$ combined with the *CC* results has confirmed the neutrino oscillation hypothesis to 30σ according to our estimate. We have obtained allowed area in parameter space and individual values for Δm^2 and $\tan^2 \theta$ with error estimation from the analysis of marginal likelihoods. We have shown that is already possible to determine at present active two neutrino oscillation parameters with relatively good accuracy. The KamLAND and specially the near future long baseline experiments will have a clear chance of first, confirming present mixing parameters obtained from solar originated neutrinos and second, measuring first and second generation mass and mixing parameters under laboratory-controlled conditions.

Acknowledgements. We acknowledge the financial support of the Italian MIUR, the Spanish CYCIT funding agencies and the CERN Theoretical Division. The numerical calculations have been performed in the computer farm of the Milano University theoretical group (THEOS).

References

- [1] Q. R. Ahmad *et al.* [SNO Collaboration], arXiv:nucl-ex/0204008.
- [2] Q. R. Ahmad *et al.* [SNO Collaboration], arXiv:nucl-ex/0204009.
- [3] Q. R. Ahmad *et al.* [SNO Collaboration], “HOWTO use the SNO solar Neutrino Spectral data”, <http://www.sno.phy.queensu.ca/sno>.
- [4] R. Davis, Prog. Part. Nucl. Phys. 32 (1994) 13. B.T. Cleveland et al., (HOMESTAKE Coll.) Nucl. Phys. (Proc. Suppl.) **B 38** (1995) 47. B.T. Cleveland et al., (HOMESTAKE Coll.) Astrophys. J. 496 (1998) 505-526.
- [5] Y. Fukuda *et al.* [Super-Kamiokande Collaboration], Phys. Rev. Lett. **82**, 2430 (1999) [arXiv:hep-ex/9812011].
- [6] Y. Fukuda *et al.* [Super-Kamiokande Collaboration], Phys. Rev. Lett. **82**, 1810 (1999) [arXiv:hep-ex/9812009].
- [7] J.N. Abdurashitov et al. (SAGE Coll.) Phys. Rev. Lett. 83(23) (1999) 4686.
- [8] P. Aliani, V. Antonelli, M. Picariello and E. Torrente-Lujan, Nucl. Phys. Proc. Suppl. **110**, 361 (2002) [arXiv:hep-ph/0112101]. P. Aliani, V. Antonelli, M. Picariello and E. Torrente-Lujan, arXiv:hep-ph/0111418.
- [9] E. Torrente-Lujan, arXiv:hep-ph/9902339. S. Khalil and E. Torrente-Lujan, J. Egyptian Math. Soc. **9**, 91 (2001) [arXiv:hep-ph/0012203].
- [10] Q. R. Ahmad *et al.* [SNO Collaboration], Phys. Rev. Lett. **87** (2001) 071301 [arXiv:nucl-ex/0106015].
- [11] S. Turck-Chieze, Nucl. Phys. Proc. Suppl. **91** (2001) 73.
E. G. Adelberger *et al.*, Rev. Mod. Phys. **70** (1998) 1265 [arXiv:astro-ph/9805121].
A. S. Brun, S. Turck-Chieze and P. Morel, arXiv:astro-ph/9806272.
- [12] J. N. Bahcall, M. H. Pinsonneault and S. Basu, Astrophys. J. **555**, 990 (2001) [arXiv:astro-ph/0010346].
- [13] J.N. Bahcall and M.H. Pinsonneault, Rev. Mod. Phys. **67** (1995) 781.
- [14] J. R. Klein [SNO Collaboration], In **Venice 1999, Neutrino telescopes, vol. 1** 115-125.
A. B. McDonald [SNO Collaboration], Nucl. Phys. Proc. Suppl. **77** (1999) 43.
- [15] J. Boger *et al.* [SNO Collaboration], Nucl. Instrum. Meth. A **449** (2000) 172 [arXiv:nucl-ex/9910016].

[16] V. Barger, D. Marfatia and K. Whisnant, Phys. Lett. B **509** (2001) 19 [arXiv:hep-ph/0104166].

[17] J. N. Bahcall, P. I. Krastev and A. Y. Smirnov, JHEP **0105** (2001) 015 [arXiv:hep-ph/0103179].

[18] Y. Fukuda *et al.* [Super-Kamiokande Collaboration], Phys. Rev. Lett. **81**, 1158 (1998) [Erratum-*ibid.* **81**, 4279 (1998)] [arXiv:hep-ex/9805021].

[19] V. Barger, D. Marfatia and K. Whisnant, arXiv:hep-ph/0106207.

[20] M. Altmann et al. (GNO Coll.) Phys. Lett. B490 (2000) 16-26.

[21] P. Anselmann et al., GALLEX Coll., Phys. Lett. **B 285** (1992) 376. W. Hampel et al., GALLEX Coll., Phys. Lett. **B 388** (1996) 384. T.A. Kirsten, Prog. Part. Nucl. Phys. **40** (1998) 85-99. W. Hampel et al., (GALLEX Coll.) Phys. Lett. **B 447** (1999) 127. M. Cribier, Nucl. Phys. (Proc. Suppl.) **B 70** (1999) 284. W. Hampel et al., (GALLEX Coll.) Phys. Lett. **B 436** (1998) 158. W. Hampel et al., (GALLEX Coll.) Phys. Lett. **B 447** (1999) 127.

[22] E. Torrente-Lujan, Phys. Rev. **D 59** (1999) 093006. E. Torrente-Lujan, Phys. Rev. **D 59** (1999) 073001. E. Torrente-Lujan, Phys. Lett. **B 441** (1998) 305. V.B. Semikoz, E. Torrente-Lujan, Nucl. Phys. **B 556** (1999) 353. E. Torrente-Lujan, Phys. Lett. **B494** (2000) 255 [hep-ph/9911458].

[23] I. Mocioiu and R. Shrock, Phys. Rev. D **62** (2000) 053017 [arXiv:hep-ph/0002149].
A. Dziewonski, in *The Encyclopedia of Solid Earth Geophysics*, edited by D.E James (Van Nostrand Reinhold, New York 1989).

[24] J. Bahcall, M. Kamionkowski, A. Sirlin, Phys. Rev. D51 (1995) 6146.

[25] S. Nakamura, T. Sato, V. Gudkov and K. Kubodera, Phys. Rev. C **63** (2001) 034617 [arXiv:nucl-th/0009012].

[26] H. Ishino, Ph. D. thesis, University of Tokio, 1999.
M. Nakahata et al. (SK Coll.), Nucl. Instrum. Methods 46 (1998) 301.

[27] M. Nakahata *et al.* [Super-Kamiokande Collaboration], Nucl. Instrum. Meth. A **421**, 113 (1999) [arXiv:hep-ex/9807027].

[28] N. Sakurai, Ph.D. Thesis, Dec. 2000 *Constraints of the neutrino oscillation parameters from 1117 day observation of solar neutrino day and night spectra in Super-Kamiokande*.

[29] G. L. Fogli and E. Lisi, Astropart. Phys. **3** (1995) 185.

- [30] S. Goswami, D. Majumdar and A. Raychaudhuri, Phys. Rev. D **63** (2001) 013003 [arXiv:hep-ph/0003163].
- [31] S. Fukuda *et al.* [Super-Kamiokande Collaboration], Phys. Rev. Lett. **86**, 5656 (2001) [arXiv:hep-ex/0103033].
- [32] S. Fukuda *et al.* [SKamiokande Collaboration], Phys. Rev. Lett. **86**, 5651 (2001) [arXiv:hep-ex/0103032].
- [33] A.I. Abazov *et al.* (SAGE Coll.), Phys. Rev. Lett. **67** (1991) 3332. D.N. Abdurashitov et al. (SAGE Coll.), Phys. Rev. Lett. **77** (1996) 4708. J.N. Abdurashitov et al., (SAGE Coll.), Phys. Rev. **C60** (1999) 055801; astro-ph/9907131. J.N. Abdurashitov et al., (SAGE Coll.), Phys. Rev. Lett. **83** (1999) 4686; astro-ph/9907113.
- [34] D. E. Groom *et al.* [Particle Data Group Collaboration], Eur. Phys. J. C **15** (2000) 1.
- [35] M. Apollonio *et al.* (CHOOZ coll.), hep-ex/9907037, Phys. Lett. **B 466** (1999) 415. M. Apollonio *et al.*, Phys. Lett. **B 420** (1998) 397.
F. Boehm *et al.*, Phys. Rev. **D62** (2000) 072002 [hep-ex/0003022].
- [36] J. Burguet-Castell and O. Mena, arXiv:hep-ph/0108109.
- [37] K. Lande (For the Homestake Coll.) Nucl. Phys. B(Proc. Suppl.)77(1999)13-19.
- [38] Y. Fukuda *et al.* [Super-Kamiokande Collaboration], Phys. Rev. Lett. **82**, 1810 (1999) [arXiv:hep-ex/9812009].
J. N. Bahcall, P. I. Krastev and E. Lisi, Phys. Rev. C **55**, 494 (1997) [arXiv:nucl-ex/9610010].
J. N. Bahcall and E. Lisi, Phys. Rev. D **54**, 5417 (1996) [arXiv:hep-ph/9607433].
J. N. Bahcall, E. Lisi, D. E. Alburger, L. De Braeckeleer, S. J. Freedman and J. Napolitano, Phys. Rev. C **54**, 411 (1996) [arXiv:nucl-th/9601044].

Experiment [Ref.]	S_{SSM}	$S_{Data}/S_{SSM} (\pm 1\sigma)$
SK (1258d) [31]	$2.32 \pm 0.03 \pm 0.08$	0.451 ± 0.011
Cl [37]	$2.56 \pm 0.16 \pm 0.16$	0.332 ± 0.056
SAGE [7, 33]	$67.2 \pm 7.0 \pm 3.2$	0.521 ± 0.067
GNO-GALLEX [20, 21]	$74.1 \pm 6.7 \pm 3.5$	0.600 ± 0.067
SNO data[1, 2]:		
CC-SNO	$1.76 \pm 0.06 \pm 0.09$	0.348 ± 0.020
ES-SNO	$2.39 \pm 0.24 \pm 0.12$	0.473 ± 0.053
NC-SNO	$5.09 \pm 0.44 \pm 0.45$	1.008 ± 0.125
$A_e(A_{TOT} \equiv 0)$ [2]	$+0.070 \pm 0.052$	

Table 1: Summary of data used in this work. The observed signal (S_{SSM}) and ratios S_{Data}/S_{SSM} with respect to the BPB2001 model are reported. The SK and SNO rates are in $10^6 \text{ cm}^{-2} \text{ s}^{-1}$ units. The Cl, SAGE and GNO-GALLEX measurements are in SNU units. In this work we use the combined results of SAGE and GNO-GALLEX: S_{Ga}/S_{SSM} ($\text{Ga} \equiv \text{SAGE}+\text{GALLEX}+\text{GNO}$)= 0.579 ± 0.050 . The SSM ${}^8\text{B}$ total flux is taken from the BPB2001 model [12]: $\phi_\nu({}^8\text{B}) = 5.05(1^{+0.20}_{-0.16}) \times 10^6 \text{ cm}^{-2} \text{ s}^{-1}$.

Method

A) Minimum LMA $\Delta m^2 = 5.44 \times 10^{-5} \text{ eV}^2$ $\tan^2 \theta = 0.40$ $\chi^2_m = 30.8$ g.o.f.: 80%

B) From Fit $\Delta m^2 = 4.5^{+2.7}_{-1.4} \times 10^{-5} \text{ eV}^2$ $\tan^2 \theta = 0.40^{+0.10}_{-0.08}$

Table 2: Mixing parameters: A) Best fit in the LMA region and B) from fit to marginal likelihood distributions.

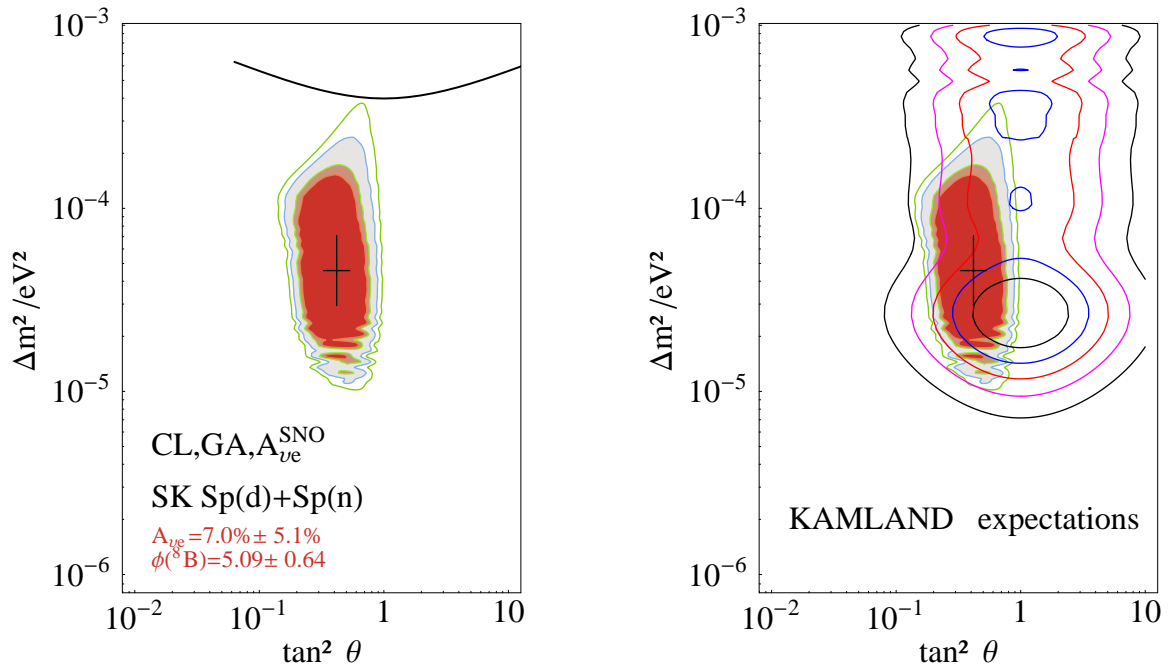


Figure 1: (Left) Allowed areas in the two neutrino parameter space. The point with error bars correspond to best the results from fit to marginal likelihoods. The colored areas are the allowed regions at 90, 95, 99 and 99.7% CL relative to the absolute minimum. The region above the upper thick line is excluded by the reactor experiments [35]. (Right) Superimposed to right figure, KamLAND constant signal contours normalized to the non-oscillation expectation. Contours, from inside to outwards, respectively at 0.4,0.5,0.6,0.7 and 0.8.

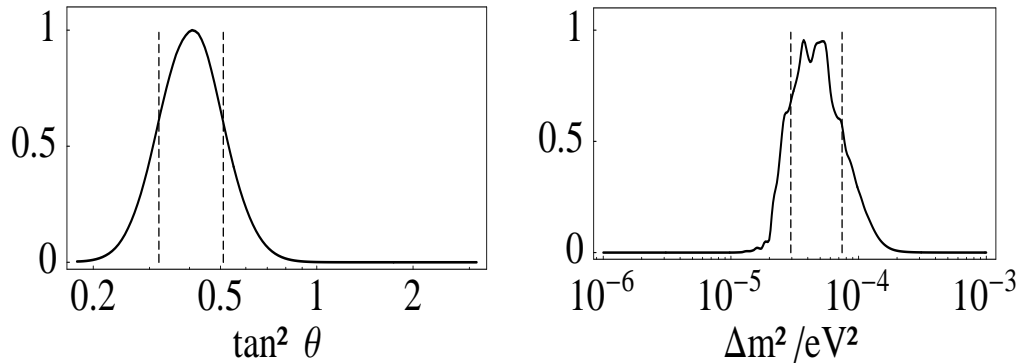


Figure 2: Marginalized likelihood distributions for each of the oscillation parameters Δm^2 (right), $\tan^2 \theta$ (left) appearing in the χ^2 fit. The curves are in arbitrary units with normalization to the maximum height. Dashed lines delimit $\pm 1\sigma$ error regions around the maximum.